

Non-Orthogonal Multiple Access for Mobile VLC Networks with Random Receiver Orientation

Yavuz Yapıcı and İsmail Güvenç

Department of Electrical and Computer Engineering, North Carolina State University, Raleigh, NC

Email: {yyapici, iguvenç}@ncsu.edu

Abstract—Visible light communications (VLC) is an emerging technology with a promise of viable solution to spectrum crunch problem in conventional radio frequency bands. In this work, we consider a VLC system where mobile users are randomly changing their horizontal location and vertical orientation. The non-orthogonal multiple access (NOMA) strategy with full channel state information (CSI) feedback is adopted to serve these users with improved spectral efficiency. To reduce computational burden and overhead due to tracking and feeding back the full CSI, we consider various limited feedback schemes where users are ordered based on their distance and vertical angle information instead of full CSI. Comprehensive numerical results verify the superiority of NOMA as compared to orthogonal multiple access while compensating the loss in user rates due to the random receiver orientation. In addition, vertical angle information based limited feedback schemes are observed to achieve satisfactory performance as compared to full CSI feedback, while conventional distance feedback scheme shows poor performance in this realistic VLC scenario.

Index Terms—Visible light communications (VLC), non-orthogonal multiple access (NOMA), random receiver orientation, user pairing, limited feedback.

I. INTRODUCTION

Visible light communications (VLC) is a promising technology for wireless 5G networks and beyond by leveraging the broad license-free optical spectrum at wavelengths of 380-750 nm [1]. Together with developments on light emitting diode (LED) as the primary illumination source, VLC networks appear as a viable solution for simultaneous illumination and communication at low power consumption and with high durability [2]. As recent research efforts reveal the power of VLC transmission being capable of achieving a speed of more than multiple Gigabits per second [3], this emerging technology enables ever increasing data-rate demanding mobile applications for next generation wireless networks.

Towards improving the performance of multiuser VLC networks even more, a recent strategy of non-orthogonal multiple access (NOMA) appears as a powerful technology suggesting to serve multiple users at the same time and frequency slot, hence in a non-orthogonal fashion [4]–[6]. The NOMA strategy has been recently considered for VLC networks with a limited attention. In [7], NOMA is considered in a VLC scenario and the performance is compared with orthogonal frequency division multiple access (OFDMA)

scheme. The performance analysis of NOMA is conducted for VLC networks in [8], [9] with various considerations involving lighting quality and power allocation. For a VLC NOMA system, a multiple-input multiple-output (MIMO) setting is explored in [10], bit-error-rate (BER) analysis is performed in [11], user sum rate maximization is conducted in [12], a location based user grouping scheme is offered in [13], and a phase pre-distorted symbol detection method is proposed in [14] with a better error performance as compared to SIC based schemes.

VLC networks involving NOMA transmission have two main drawbacks which are the overhead of full CSI feedback and availability of line-of-sight (LOS) links. Since the NOMA transmitter needs to order users according to their channel qualities, the channel gains should be estimated at user side and fed back to the transmitter, which causes computational burden while tracking unknown channel gains, and link overheads during feeding back this information. In addition, VLC transmission highly relies on LOS links, which may not be readily available all the time, especially when the receiving direction towards LED is outside the field-of-view (FOV) of the receiver. The problem of LOS link unavailability naturally arises in VLC networks with mobile users because of random user orientations around receiving direction, which is rigorously handled in [15], [16].

In this paper we consider a multiuser VLC network, where mobile users with varying locations are served by NOMA transmission with various full and limited feedback schemes, and the receiver direction is changing randomly in the vertical plane. To the best of our knowledge, this realistic VLC scenario has not been studied in the literature before. We investigate the performance of NOMA with ideal full CSI feedback as well as various limited feedback schemes involving distance and vertical angle information. We show through comprehensive numerical results that NOMA is superior to conventional orthogonal multiple access (OMA) while compensating the loss in user rates due to the random orientation of VLC receivers. Furthermore, we show that the vertical angle based limited feedback schemes can achieve a satisfactory level of user rates as compared to full CSI feedback. Because of the unique feature of this realistic VLC network (with random receiver orientation), distance only feedback scheme falls short of angle based alternatives although distance feedback is a reasonable candidate for radio frequency (RF) networks [17].

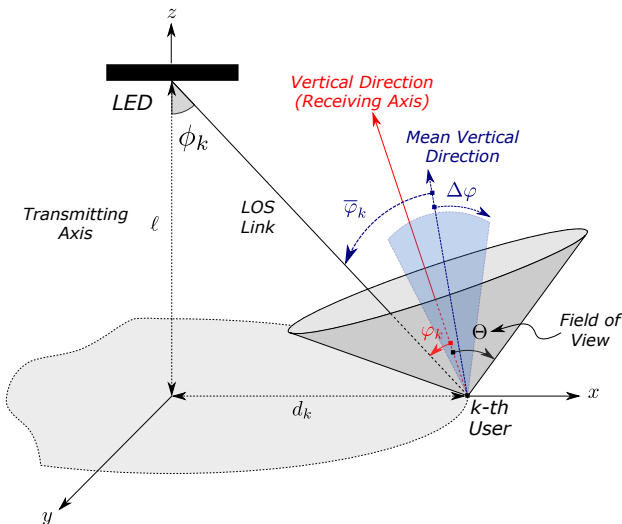


Fig. 1: Multiuser VLC network showing k th user explicitly.

The rest of the paper is organized as follows. Section II introduces the system model. Section III considers the NOMA transmission with various feedback schemes. Section IV presents the numerical results and Section V concludes the paper with some final remarks.

Notations: $\mathcal{U}[a, b]$ denotes the continuous uniform distribution over the interval $[a, b]$. $\delta(i, j)$ is Kronecker delta taking 1 if $i = j$, and 0 otherwise.

II. SYSTEM MODEL

We consider an indoor VLC downlink transmission scenario involving a single transmitting LED and K users each of which is equipped with a receiving photodetector. The interaction between the LED and k th user over a LoS link is depicted in Fig. 1. The corresponding direct current (DC) channel gain is given as

$$h_k = \frac{(m+1)A_r}{2\pi(\ell^2 + d_k^2)} \cos^m(\phi_k) \cos(\varphi_k) \Pi[\varphi_k/\Theta], \quad (1)$$

where ℓ is the vertical distance between the LED and the plane including all the users, d_k is the horizontal distance of the k th user to the LED, ϕ_k and φ_k are the angle of irradiance and incidence of the k th user, respectively, $m = -1/\log_2(\cos(\Phi))$ is the Lambertian order with Φ being the half-power beamwidth of the LED, A_r and Θ are the detection area and field of view (FOV) of the photodetectors. The notation $\Pi[x]$ represents a rectangular function given as

$$\Pi[x] \triangleq \begin{cases} 1 & \text{for } |x| \leq 1 \\ 0 & \text{for } |x| > 1 \end{cases}, \quad (2)$$

and, hence, the channel gain of the k th user is nonzero only if φ_k is smaller than Θ , or equivalently LED is inside the receiver FOV.

We assume that the users are non-stationary within both the horizontal and vertical planes such that they are continuously changing their locations and orientations. In particular, the horizontal distance d_k of k th user (representing the location

in the horizontal plane) is assumed to follow a uniform distribution with $\mathcal{U}[d_{\min}, d_{\max}]$ m. In addition, the vertical orientation of k th user is also varying around a *mean vertical angle* $\bar{\varphi}_k$, which is picked up from a uniform distribution with $\mathcal{U}[\bar{\varphi}_{\min}, \bar{\varphi}_{\max}]$, within a maximum deviation angle of $\Delta\varphi$. As a result, the k th user's orientation or, equivalently, the *vertical angle* φ_k takes a value from a uniform distribution with $\mathcal{U}[\bar{\varphi}_k - \Delta\varphi, \bar{\varphi}_k + \Delta\varphi]$.

Furthermore, we assume that the distance d_k , mean vertical angle $\bar{\varphi}_k$, and vertical angle φ_k of k th user do not change during a single transmission period over which the respective user rates are evaluated. In subsequent transmission periods, all these variables take new values from their respective distributions, where we assume that d_k and $\bar{\varphi}_k$ are varying much slowly as compared to φ_k , and, hence, have relatively large coherence time. As a result, each user is changing its location and mean vertical direction slowly, although relatively small variations in actual vertical angle happen much quickly. Hence, d_k and $\bar{\varphi}_k$ are good candidates for limited feedback schemes since they can be tracked with less computational burden. In the meanwhile, any limited feedback scheme involving d_k or $\bar{\varphi}_k$ only will degrade the user rates since they do not capture the status of the receiver direction being inside or outside the FOV, which we call *FOV status* and represented by $\Pi[\theta_k/\Theta]$ in (1). In the next section, we will consider this compromise between limited feedback (with lower computational burden and overhead) and better user rates during the NOMA transmission.

III. NON-ORTHOGONAL MULTIPLE ACCESS

In this section, we investigate the details of the NOMA transmission for the VLC downlink setting presented in Section II with a special attention to full CSI and some low-rate limited feedback schemes.

A. NOMA Transmission and User Rates

In NOMA transmission, multiple users of sufficiently different channel qualities are served simultaneously in the same frequency band, which results in a non-orthogonal transmission strategy. The respective messages of users paired for NOMA transmission, which are therefore referred to as NOMA users, are weighted by suitable power allocation coefficients each of which is inversely proportional to the channel quality of respective NOMA user, as sketched in Fig. 2. The weighted messages are then combined together along with the superposition coding principle, and sent to all users. Each NOMA user decodes its own message after decoding, if any, messages of relatively weaker users allocated with more power, while treating the messages of stronger users as noise. In the meanwhile, the decoded messages of weaker users are cancelled from the received signal through successive interference cancellation (SIC) approach.

Without any loss of generality, we assume that j th user has the j th largest nonzero channel gain among L users involved in NOMA transmission with $L < K$. The SINR at j th user while

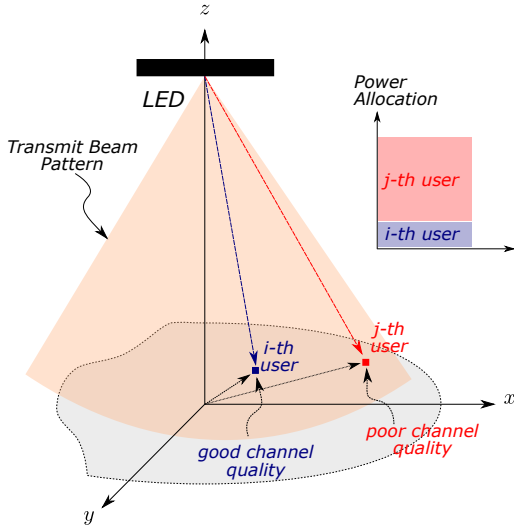


Fig. 2: VLC NOMA transmission with 2 users where i th and j th users are the weaker and stronger ones, respectively.

decoding the message of a weaker i th user with $i < j \leq L$ is given as

$$\text{SINR}_{i \rightarrow j} = \frac{h_j^2 \beta_i^2}{h_j^2 \sum_{k=i+1}^K \beta_k^2 + \gamma^{-1}}, \quad (3)$$

where β_k is the power allocation coefficient of k th user such that $\sum_{k=1}^K \beta_k^2 = 1$, and γ is the transmit signal-to-noise ratio (SNR). Note that (3) implicitly assumes that the message of any k th user with $k < i$ and, hence, having a weaker channel gain than that of i th user has already been decoded successfully and subtracted from the received signal as per SIC strategy. Furthermore, SINR of j th user while decoding its own message is defined as

$$\text{SINR}_j = \frac{h_j^2 \beta_j^2}{(1 - \delta(j, L)) h_j^2 \sum_{k=j+1}^K \beta_k^2 + \gamma^{-1}}. \quad (4)$$

At any NOMA user, the overall decoding mechanism is assumed to be in outage if instantaneous user rates associated with either of (3) or (4) do not meet the respective target rates of NOMA users based on their preset quality-of-service (QoS) requirements. In particular, assuming $R_{i \rightarrow j} = \log_2(1 + \text{SINR}_{i \rightarrow j})$ and $R_j = \log_2(1 + \text{SINR}_j)$ are instantaneous rates associated with (3) and (4), respectively, outage probability of j th user is defined as

$$P_j^o = 1 - \Pr \left(R_{1 \rightarrow j} > \bar{R}_1, \dots, R_{j-1 \rightarrow j} > \bar{R}_{j-1}, R_j > \bar{R}_j \right), \quad (5)$$

where \bar{R}_k is the QoS based target rate of k th user. Defining $\epsilon_k = 2^{\bar{R}_k} - 1$, outage probability in (5) is given in terms of SINR as follows

$$P_j^o = 1 - \Pr \left(\text{SINR}_{1 \rightarrow j} > \epsilon_1, \dots, \text{SINR}_{j-1 \rightarrow j} > \epsilon_{j-1}, \text{SINR}_j > \epsilon_j \right), \quad (6)$$

and, the respective sum rate is accordingly defined as

$$R^{\text{NOMA}} = \sum_{k=1}^L (1 - P_k^o) \bar{R}_k. \quad (7)$$

For the OMA transmission, we assume that all resources are allocated to a single user while it is served equally during $1/L$ of the total transmission period, hence results in the following sum rate expression

$$R^{\text{OMA}} = \sum_{k=1}^L \left[1 - \Pr \left(|h_k|^2 < \eta_k \right) \right] \bar{R}_k, \quad (8)$$

where $\eta_k = 2^{L\bar{R}_k} - 1$.

B. Optimal and Low-Rate Feedback Schemes

In NOMA transmission, users to be served are chosen among a total of K users based on their relative channel qualities. It is therefore vital for NOMA transmitter to order users according to their channel qualities based on the information fed back from users. The optimal strategy from this perspective is to order users according to their full CSI as follows

$$|h_1|^2 < |h_2|^2 < \dots < |h_K|^2, \quad (9)$$

where we label the user having the k th stronger channel gain as k th user, without any loss of generality.

Because the channel gains need to be tracked continuously to enable full CSI feedback, some limited feedback alternatives on channel qualities are considered to relieve computational complexity at user side. To this end, we investigate three different limited feedback schemes (instead of full CSI feedback), which involve distance d_k , vertical angle φ_k , and mean vertical angle $\bar{\varphi}_k$ information separately, and result in the following ordered user sets

$$|h_{d,1}|^2 < |h_{d,2}|^2 < \dots < |h_{d,K}|^2, \quad (10)$$

$$|h_{\varphi,1}|^2 < |h_{\varphi,2}|^2 < \dots < |h_{\varphi,K}|^2, \quad (11)$$

$$|h_{\bar{\varphi},1}|^2 < |h_{\bar{\varphi},2}|^2 < \dots < |h_{\bar{\varphi},K}|^2, \quad (12)$$

respectively. The respective partial channel gain expressions in these limited feedback based orders are obtained using (1) and available feedback information as follows

$$h_{d,k} = \frac{(m+1)A_r}{2\pi} \ell^m (\ell^2 + d_k^2)^{-\frac{m+2}{2}}, \quad (13)$$

$$h_{\varphi,k} = \frac{(m+1)A_r}{2\pi} \cos(\varphi_k) \Pi[\varphi_k/\Theta], \quad (14)$$

$$h_{\bar{\varphi},k} = \frac{(m+1)A_r}{2\pi} \cos(\bar{\varphi}_k) \Pi[\bar{\varphi}_k/\Theta], \quad (15)$$

where (13) is obtained by substituting the geometrical equivalent of $\cos^m(\phi_k)$ according to the setting in Fig. 1.

Remark 1: Since distance based feedback scheme does not involve angle information, respective partial channel gain in (13) does not perform any check regarding FOV status (whether the receiving direction is inside FOV or not). As we present in Section IV, the lack of angle information and, hence, FOV status check in distance feedback scheme results

in degraded user rates since receiver direction is changing randomly in the vertical plane. It is therefore more convenient to consider angle based feedback schemes when the receiver orientation is random, which improves achievable rates by incorporating FOV status into user ordering, as shown in (14) and (15) via the function $\Pi[\cdot]$.

Remark 2: The coherence time of the receiver orientation captured by the vertical angle φ_k can be anticipated to be much less than that for the horizontal distance d_k (representing geometrical position), and, hence, it should be estimated more frequently. Although this discussion might bring up some doubt regarding the feasibility of vertical angle based feedback, the mean vertical angle $\bar{\varphi}_k$ can be reasonably assumed to be changing much slowly, and, hence, $\bar{\varphi}_k$ appears as a powerful alternative for limited feedback schemes since it relieves the computational burden by requesting update for its value less frequently.

IV. NUMERICAL RESULTS

We assume a total of $K=20$ users, which are randomly deployed over a plane where the horizontal distance d_k follows a uniform distribution with $\mathcal{U}[0,5]$ m. The vertical angle φ_k and mean vertical angle follow uniform distribution with $\mathcal{U}[\bar{\varphi}_k - \Delta\varphi, \bar{\varphi}_k + \Delta\varphi]$ and $\mathcal{U}[\bar{\varphi}_{\min}, \bar{\varphi}_{\max}]$, respectively, where $\bar{\varphi}_{\min} = 10^\circ$, $\bar{\varphi}_{\max} = 90^\circ$, and $\Delta\varphi = 10^\circ$ unless otherwise stated. We assume that the LED is vertically off the horizontal plane including all the users by $\ell = 2$ m with a half power beamwidth of $\Phi_{\text{HPBW}} = 60^\circ$, the receiver area of the photodetector is $A_e = 1 \text{ cm}^2$, and FOV of the receiver is $\Phi_{\text{FOV}} = 60^\circ$.

We choose two users at a time ($L=2$) for NOMA transmission based on channel qualities as described in Section III-B. In particular, we label i th and j th users as the weaker and the stronger ones, respectively, where $i=1$ and $j=10$. We assume that respective power coefficients are $\beta_i = 15/16$ and $\beta_j = 1/16$, while the target data rates are $\bar{R}_i = 2 \text{ bit/s/Hz}$ and $\bar{R}_j = 10 \text{ bit/s/Hz}$.

The sum rates for NOMA transmission with random receiver orientation are depicted in Fig. 3 for full CSI feedback as well as the limited feedback of distance, vertical angle, and mean vertical angle only cases. For comparison purposes, sum rates for NOMA transmission with fixed receiver orientation, where all the receivers are looking up directly towards ceiling, and OMA transmission with random receiver orientation are also provided assuming full CSI feedback. We observe that the random receiver orientation with even a small vertical deviation of $\Delta\varphi = 10^\circ$ causes 10 dB more transmit power to achieve the maximum sum rate of 12 bit/s/Hz, when the NOMA strategy with full CSI feedback is adopted. The respective sum rate of OMA is observed to achieve the same maximum sum rate with 25 dB more transmit power as compared to NOMA, which highlights NOMA as a powerful candidate while dealing with adverse effects of random receiver orientation.

When we consider computationally more efficient feedback alternatives for NOMA, vertical angle information performs the best among the others where it attains the maximum achievable sum rate at a transmit power of 15 dB off NOMA

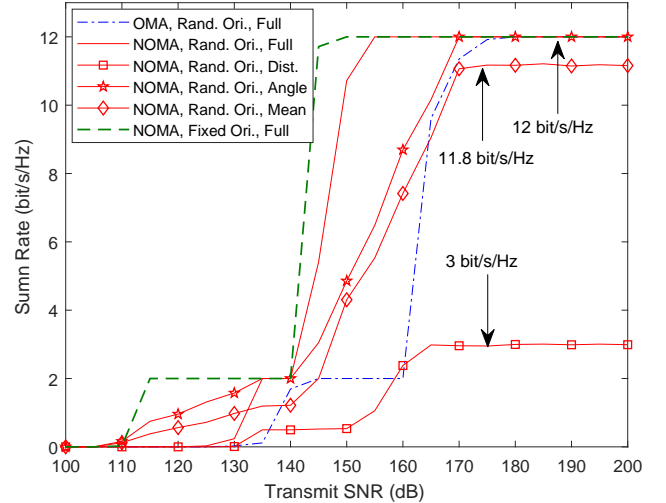


Fig. 3: Sum rates of OMA and NOMA transmission for fixed and random receiver orientations with feedback schemes of full CSI, distance, vertical angle, and mean vertical angle.

with the full CSI feedback, and outperforms OMA with full CSI feedback. When we relax the angle information by feeding back the mean vertical angle only, which relieves the burden of tracking the angle information for mobile users, the respective sum rate is now away from the exact vertical angle case by 2 dB and saturates at 11.2 bit/s/Hz. Hence, the degradation in sum rate with respect to maximum achievable level is only 7% when mean of the vertical angle values are employed. The distance feedback is observed to perform the worst of all, and the resulting sum rate saturates at a very small value of 3 bit/s/Hz only (25% of the maximum achievable sum rate), which can be considered as the cost of not involving vertical angle information and, hence, FOV status check, and is far below the mean vertical angle feedback case.

As a remark, sum rates for two variants of limited angle feedback are higher than that for the full CSI feedback at low transmit power, which seems interesting. In this low power regime, the stronger (j th) user is always in outage as shown in Fig. 4, and the benefit of NOMA should, therefore, not be expected for this single user transmission case. Note that weaker (i th) user can always be served better in this regime as i gets larger (channel quality improves), and this is what the angle feedback variants unintentionally do whenever the respective user ordering does not match that of the full CSI feedback. In Fig. 5, we depict the probability histogram of *actual order* of the weaker user for angle and mean angle feedback schemes assuming a transmit SNR of 130 dB and $i=1$. The actual order represents the order of the weaker user with respect to the full CSI, where the weaker user appears as the i th largest one when the channel qualities are ordered based on vertical or mean vertical angle information. Note that we order only the nonzero channel quantities, and zero actual order value in Fig. 5 represents the cases where the i th user of

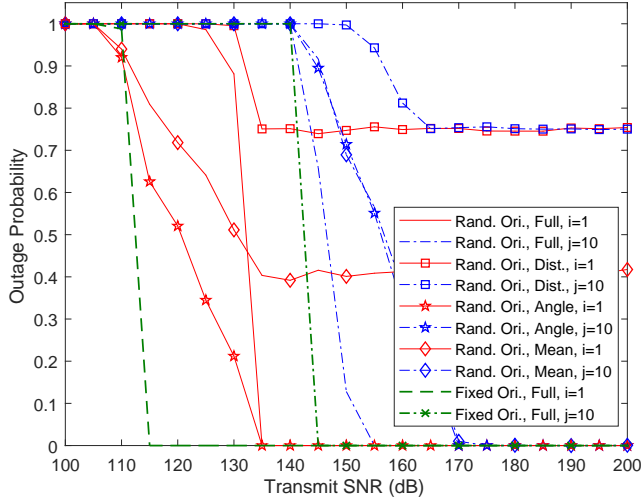


Fig. 4: Outage probabilities of OMA and NOMA for fixed and random receiver orientations with feedback schemes of full CSI, distance, vertical angle, and mean vertical angle.

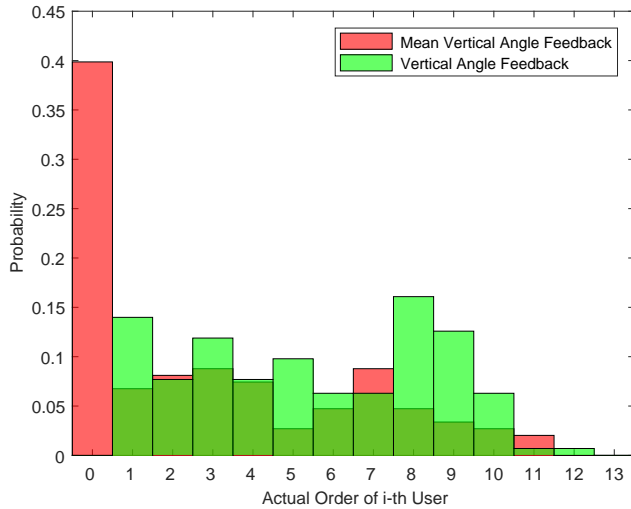


Fig. 5: Actual order of the weaker user for NOMA transmission with random receiver orientation and $i=1$ assuming a transmit power of 130 dB.

mean vertical angle feedback is actually outside the FOV and, hence, corresponds to a full CSI value of zero. We observe that the actual order of i th user can take values $i > 1$, which means better channel quality as compared to $i=1$ case, and is therefore the reason for a better outage and sum rate at low power regime.

The respective outage probabilities are depicted in Fig. 4 for the stronger and weaker users separately. Considering the outage for fixed receiver orientation for both users, the random vertical orientation with full CSI feedback is observed to cause a loss only in diversity order (slope of the curves) for the

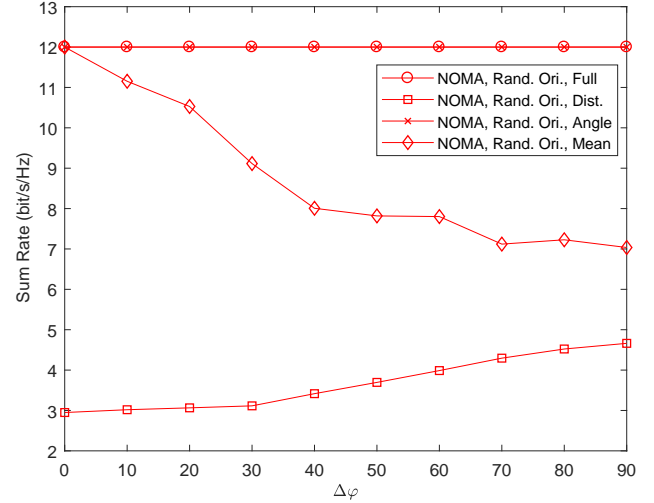


Fig. 6: Sum rates of NOMA with random receiver orientations for varying deviation angle $\Delta\varphi$ assuming a transmit power of 180 dB and feedback schemes of full CSI, distance, vertical angle, and mean vertical angle.

stronger j th user, whereas the weaker i th user experiences degradation both in diversity order and transmit SNR of as large as 20 dB. We observe that while the feedback of distance information results in a saturation at 0.75 for both users, the mean vertical angle causes saturation for only the weaker i th user and at a lower probability value of 0.4. Note that, any saturation in outage probabilities reflects itself as the degradation in sum rates not achieving the maximum possible value of 12 bit/s/Hz in our particular case, as shown in Fig. 3.

Finally, we plot sum rates for varying deviation angles $\Delta\varphi$ in Fig. 6 assuming a transmit power of 180 dB. We observe that the feedback of vertical angle is very robust to deviation angle values since it captures the status of the receiver direction being inside or outside the FOV, which is previously referred to as FOV status, perfectly. As the receiver orientation changes more, which is represented by larger deviation angle values, the performance of mean angle feedback degrades since it becomes more likely to have a different FOV status than that of the actual receiver direction. Nevertheless, mean angle feedback is still superior to distance feedback, even at an extreme deviation of $\Delta\varphi = 90^\circ$. Note that, the weaker and stronger users chosen based on distance information are more likely to have a nonzero channel value as the deviation angle $\Delta\varphi$ increases, which is the reason for increasing sum rate of distance feedback in Fig. 6, although $\Delta\varphi > 30^\circ$ might be mostly considered as of theoretical importance.

V. CONCLUSION

We consider a multiuser VLC network involving mobile users with random location and vertical orientation. In order to improve spectral efficiency, NOMA is considered with full CSI feedback as well as distance (location) and vertical angle

information based limited feedback schemes. We observe that NOMA is superior to OMA while compensating loss in user rates due to the random vertical orientation, and that angle based feedback schemes can achieve a satisfactory performance. We also observe that distance based feedback scheme achieves a poor user rate performance because of random user orientation, which result in saturation at a rate much lower than the maximum achievable sum rate.

REFERENCES

- [1] A. Jovicic, J. Li, and T. Richardson, "Visible light communication: Opportunities, challenges and the path to market," *IEEE Commun. Mag.*, vol. 51, no. 12, pp. 26–32, Dec. 2013.
- [2] H. Burchardt, N. Serafimovski, D. Tsonev, S. Videv, and H. Haas, "VLC: Beyond point-to-point communication," *IEEE Commun. Mag.*, vol. 52, no. 7, pp. 98–105, Jul. 2014.
- [3] D. Tsonev, H. Chun, S. Rajbhandari, J. J. D. McKendry, S. Videv, E. Gu, M. Haji, S. Watson, A. E. Kelly, G. Faulkner, M. D. Dawson, H. Haas, and D. O'Brien, "A 3-Gb/s Single-LED OFDM-Based Wireless VLC Link Using a Gallium Nitride μ LED," *IEEE Photonics Technology Letters*, vol. 26, no. 7, pp. 637–640, Apr. 2014.
- [4] Z. Ding, Y. Liu, J. Choi, Q. Sun, M. Elkashlan, C. L. I, and H. V. Poor, "Application of non-orthogonal multiple access in LTE and 5G networks," *IEEE Commun. Mag.*, vol. 55, no. 2, pp. 185–191, Feb. 2017.
- [5] W. Shin, M. Vaezi, B. Lee, D. J. Love, J. Lee, and H. V. Poor, "Non-orthogonal multiple access in multi-cell networks: Theory, performance, and practical challenges," *IEEE Communications Magazine*, vol. 55, no. 10, pp. 176–183, OCTOBER 2017.
- [6] S. M. R. Islam, N. Avazov, O. A. Dobre, and K. s. Kwak, "Power-domain non-orthogonal multiple access (NOMA) in 5G systems: Potentials and challenges," *IEEE Commun. Surveys Tuts.*, vol. 19, no. 2, pp. 721–742, 2nd Quarter 2017.
- [7] R. C. Kizilirmak, C. R. Rowell, and M. Uysal, "Non-orthogonal multiple access (NOMA) for indoor visible light communications," in *Int. Workshop on Optical Wireless Commun. (IWOW'2015)*, Sep. 2015, pp. 98–101.
- [8] L. Yin, W. O. Popoola, X. Wu, and H. Haas, "Performance evaluation of non-orthogonal multiple access in visible light communication," *IEEE Trans. Commun.*, vol. 64, no. 12, pp. 5162–5175, Dec. 2016.
- [9] H. Marshoud, V. M. Kapinas, G. K. Karagiannidis, and S. Muhaidat, "Non-orthogonal multiple access for visible light communications," *IEEE Photon. Technol. Lett.*, vol. 28, no. 1, pp. 51–54, Jan. 2016.
- [10] C. Chen, W. D. Zhong, H. Yang, and P. Du, "On the performance of MIMO-NOMA based visible light communication systems," *IEEE Photon. Technol. Lett.*, vol. PP, no. 99, pp. 1–1, Dec. 2017.
- [11] H. Marshoud, P. C. Sofotasios, S. Muhaidat, G. K. Karagiannidis, and B. S. Sharif, "On the performance of visible light communication systems with non-orthogonal multiple access," *IEEE Trans. Wireless Commun.*, vol. 16, no. 10, pp. 6350–6364, Oct. 2017.
- [12] Z. Yang, W. Xu, and Y. Li, "Fair non-orthogonal multiple access for visible light communication downlinks," *IEEE Wireless Commun. Lett.*, vol. 6, no. 1, pp. 66–69, Feb. 2017.
- [13] X. Zhang, Q. Gao, C. Gong, and Z. Xu, "User grouping and power allocation for NOMA visible light communication multi-cell networks," *IEEE Commun. Lett.*, vol. 21, no. 4, pp. 777–780, Apr. 2017.
- [14] X. Guan, Q. Yang, and C. K. Chan, "Joint detection of visible light communication signals under non-orthogonal multiple access," *IEEE Photon. Technol. Lett.*, vol. 29, no. 4, pp. 377–380, Feb. 2017.
- [15] Y. S. Eroglu, Y. Yapici, and I. Güvenç, "Impact of random receiver orientation on visible light communications channel," under review in *J. Lightw. Technol.*, Oct. 2017. [Online]. Available: <http://arxiv.org/abs/1710.09764>
- [16] —, "Effect of random vertical orientation for mobile users in visible light communications," in *Proc. Asilomar Conf. Signals, Syst., and Comput.*, Pacific Grove, California, Oct. 2017.
- [17] Z. Ding, P. Fan, and H. V. Poor, "Random beamforming in millimeter-wave NOMA networks," *IEEE Access*, vol. 5, pp. 7667–7681, Feb. 2017.